Molecular-dynamics study of collision, implantation, and fragmentation of Ag_7 on Pd(100)

Giovanna Vandoni, Christian Félix, and Carlo Massobrio*
Institut de Physique Expérimentale, Ecole Polytechnique Fédérale de Lausanne, CH-1015 Lausanne, Switzerland
(Received 21 July 1995; revised manuscript received 18 March 1996)

By using embedded-atom-method interatomic potentials and molecular-dynamics simulations, we study the collision of a single Ag_7 cluster on the Pd(100) substrate, at impact energies in the direction perpendicular to the (100) surface $E_1=20$ eV (2.86 eV/atom) and $E_2=95$ eV (13.6 eV/atom). Our results indicate that implantation occurs at both impact energies, but it is more important at E_2. As opposed to what is shown experimentally, little fragmentation takes place for E_1, while the calculated cluster fragmentation is in good agreement with the experimental data for E_2. [S0163-1829(96)08224-0]

I. INTRODUCTION

The primary purpose of mass-selected cluster deposition on solid surfaces, carried out at incidence energies as small as a few eV per atom (cluster ''soft landing''), is to investigate the cluster behavior in the environment provided by the substrate, while attempting to minimize irreversible structural changes occurring at much higher impact energies. Efforts in this direction have recently allowed the experimental elucidation of the outcome of mass-selected depositions of Ag_7^+ on Pd(100) at incidence energies of $E_1=20$ eV (2.86 eV/atom) and $E_2=95$ eV (13.6 eV/atom), by using thermal energy atom scattering (TEAS).[1] In Ref. 1, the cluster cross sections for diffuse scattering, obtained from the attenuation of the helium specular intensity, have been reported for the two impact energies E_1 and E_2 as a function of surface temperature in the range $80<T<400$ K. Even though these cross sections cannot reveal the identities of the collision products, they are sensitive to the shape of the adsorbates and can be exploited to obtain information on their nature, i.e., their dimensional character as well as the extent of fragmentation, implantation, and defect production on the substrate. In order to extract this information, a simple model based on enhanced fragmentation of clusters at both impact energies and implantation of Ag atoms into the outer layers has been proposed in Ref. 1. This model was found to be consistent with the behavior of the cross section as a function of temperature, suggesting that cluster fragmentation can hardly be avoided in ''soft landing'' deposition experiments on solid surfaces, where implantation and site exchanges between cluster and substrate atoms already occur at low impact energy.

A useful tool to complement the TEAS approach is represented by atomic scale simulations. Recent investigations of this kind[2–4] have provided a wealth of information on the dynamical and structural rearrangements brought about by the energetic deposition. Furthermore, they have been found compatible with the interpretation of the TEAS data given in Ref. 1.

In this work the Ag_7^+/Pd(100) deposition process is investigated via molecular-dynamics simulations of the collision of a single Ag_7 cluster on the Pd(100) substrate. Within the limits of a temporal evolution restricted to some ps, our simulations aim at providing a direct view of what happens to the cluster atoms and their substrate neighbors as a result of the collision in the low-temperature range. Moreover, the comparison between experimental and simulation results can be useful to check the overall adequacy of the microscopic model employed with respect to the physical process under consideration.

II. MODEL AND COMPUTATIONS

Our simulations are based on the parametrization of the embedded-atom potentials for Ag and Pd given in Ref. 5, with cutoff radii equal to 5.25 Å. As suggested in Ref. 2, we found it appropriate to replace the embedded-atom-method (EAM) two-body, repulsive part of the potentials, with a Molière potential[6] in the range of distances up to $r_1=0.9$ Å, while a third-order polynomial matches the Molière and the EAM repulsive potentials at $r_1=0.9$ Å and $r_2=1.9$ Å, respectively. The embedding functions of the EAM potential are set smoothly to zero at values of the EAM bulk electronic density corresponding to bulk distances 85% shorter than the zero pressure equilibrium value. The Ag-Ag repulsive potential is further modified by adding an interaction E_R of the kind $E_R=A\exp[-(r-r_d)\lambda]$, where A, λ, and r_d are fitted to the cohesive energies ($E_c=1.71$ eV) and average equilibrium distance of the Ag_7 ground-state structure ($d_c=2.81$ Å) obtained via quantum-chemical configuration interaction calculations.[7] The best fit is obtained with the parameters $A=0.28$ eV, $r_d=2.8$ Å, $\lambda=12$ Å^{-1}, yielding $E_c=1.71$ eV and $d_c=2.88$ Å. Our description of an isolated small Ag cluster by using effective potentials is in principle questionable, since it does not account for electronic effects crucial to reproduce correctly their structural properties. Nevertheless, it is more legitimate in the context of cluster deposition on surfaces,[8–11] since we focus here on the main features of processes involving cluster atoms in interaction with substrates.

In our calculations the Pd(100) system is a periodic slab made of ten atomic layers defining the X [010] and Y [001] directions, each layer containing 128 atoms. Prior to the simulation of the collision events, the slab is relaxed at $T=0$ K. The impact of Ag_7 on Pd(100) is simulated at perpendicular incidence with respect to the surface plane (initial velocity directed along [100]) or by introducing an angle $\vartheta=15°$ or 35° with respect to the surface normal. For both normal

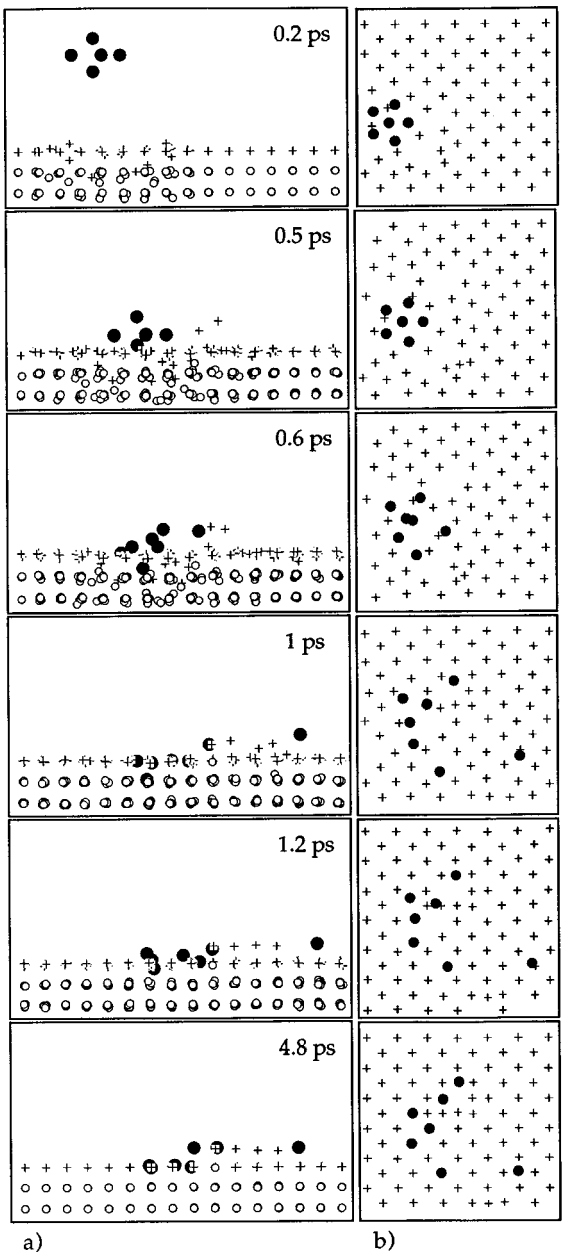

FIG. 1. Collision sequence of a Ag heptamer with Pd(100), at 95 eV total kinetic energy in the perpendicular direction (along the z axis) and 15° incidence. Black circles represent Ag atoms, crosses are Pd atoms of the first layer, and white circles are Pd atoms of the second and third layer. In (a), the atoms are shown with coordinates projected onto the xz plane; in (b), with coordinates projected onto the xy plane.

and non-normal incidence, the total initial kinetic energy along the Z direction is taken to be either $E_1=20$ eV or $E_2=95$ eV. This choice is consistent with the ''soft landing'' experiment of Ref. 1, where the cluster's mean angle of incidence is 15°, and only the normal component of the velocity is limited by the retarding potential applied to the crystal. Throughout the calculations, the bottom layer of the Pd(100) slab is kept at very low temperatures by use of a dynamical thermostat in order to mimic the flow of thermal energy induced by the impact and avoid artificial heating up of the system due to its limited size. This limits the comparison

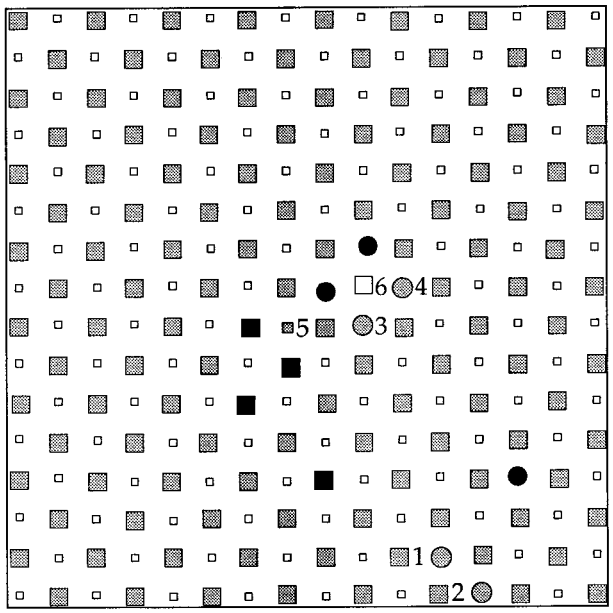

FIG. 2. Final location of cluster and substrate atoms, in the collision event illustrated above. Black symbols: Ag atoms; shadowed symbols: Pd atoms originally in the first layer, white symbols: Pd atoms originally in the second layer. For both Ag and Pd, circles represent adatoms, big squares represent atoms of the first layer, and small squares are atoms in the second layer.

with experiments to the lowest temperature considered in Ref. 1, $T=80$ K. Overall, a few hundred collision events are produced, by varying impact energy, incidence angle, impact parameter, and orientation of the cluster with respect to the substrate.

III. RESULTS

A collision event at high energy is illustrated in Figs. 1(a) and 1(b). In this case, the cluster is given an initial kinetic energy $E_2=95$ eV in the perpendicular direction, and 6.65 eV in the parallel direction, resulting in an angle of incidence of 15°. The figure shows snapshots of the atomic positions during the collision. The coordinates recorded after 4.8 ps (shown in the bottom panel) reflect the long time behavior, with both cluster and substrate atoms frozen in their final positions. During the first 0.5 ps, the cluster remains essentially entire, even if some disorder is created in the substrate. Later on, the cluster atoms are found to be significantly farther apart from each other. Some atoms penetrate into the substrate as deeply as in the second layer, some remain in the adlayer. After 1 ps, the implanted cluster atoms rebound upwards, and eventually all the cluster atoms start to relax into substitutional sites, either in the first layer or in the adlayer. The final locations of the cluster and substrate atoms are summarized in Fig. 2. Only three Ag atoms remain in the adlayer, whereas four are implanted in substitutional sites in the first layer. Concerning the substrate, four Pd adatoms (labeled 1–4 in Fig. 2) are created, and one atom from the first layer (5) is implanted in the second layer, ejecting in turn one atom (6) in the first layer. Both Ag and Pd adatoms are scattered over a large surface region.

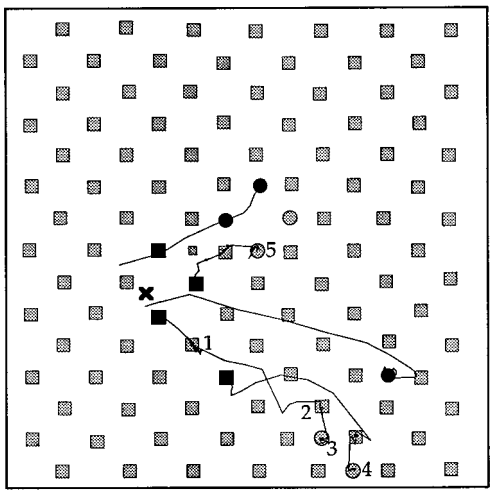

FIG. 3. Trajectories described by some of the Pd atoms relocated by the collision events illustrated in Fig. 1, and by some of the Ag atoms. Symbols have the same meaning as in Fig. 2. The cross marks the impact point of the center of mass of the cluster on the surface. Three replacement sequences are visible. In the lower part of the figure, a Ag atom is implanted into the first layer, substituting the Pd atom labeled 1, which in turn takes the place of atom 2; the latter channels inside the first layer and finally replaces and ejects atom 3. Two further replacement sequences produce the Pd adatoms labeled 4 and 5. Also displayed are the trajectories of the two Ag adatoms, which come to rest at the greatest distance from the impact point.

The reasons for this wide outspread are easily understood by studying the trajectories presented in Fig. 3. The Pd adatoms are created at some distance from the impact point by short replacement collision sequences, which involve atoms from the first layer, and can therefore be considered as surface focused. One of the implanted Ag atoms substitutes a Pd atom from the first layer, which collides and takes the place of a second one, which in turn substitutes and ejects into the adlayer a third Pd atom. Figure 3 shows three such replacement collision sequences, which are responsible for the creation of Pd adatoms labeled 3–5. Some Ag adatoms experience transient mobility before coming to rest. Indeed, it appears that the two Ag adatoms which are located at the greatest distance from the impact point have channeled on the surface along high symmetry directions, coming to equilibrium at several lattice sites from the original center of mass of the cluster. A global picture of the collision process can be obtained by studying the results of the simulations averaged over several events. Table I gives the average number of Ag atoms in the adlayer and the first three surface layers as a function of energy and incidence angle, extracted from 45 simulated collisions. Both the probability and the depth of implantation strongly depend on energy. At E_1, no Ag atoms are found below the first layer at the end of the simulation. On the average, at most 1.7 atoms are implanted in the first layer. On the other hand, at E_2, Ag atoms substitute Pd atoms even in the third layer, and only less than half of the cluster atoms remain in the adlayer. We notice that by increasing ϑ, the implantation probability is strongly attenuated. We recall that an increased value of ϑ does not modify the velocity of the cluster in the Z direction, while it increases the velocity component in the direction parallel to the surface. The average number of surface defects produced by the collisions is also displayed in Table I. It is interesting to notice that the number of Pd adatoms corresponds to the number of Ag substitutional impurities at low energy and that no vacancies are produced, whereas increasing the energy results in an increased number of Pd adatoms, as well as in the production of vacancies. This feature confirms that more disorder is created at higher energy.

TABLE I. Depth distribution of Ag substitutional impurities and average number of defects produced in the surface layer (Pd adatoms and vacancies) as a function of incidence energy and angle. We recall that at E_2=95 eV and 15° incidence, backscattering is observed in four cases in 45 simulated collisions. The last three rows illustrate the fragmentation of the cluster, described by the parameter $\langle r \rangle$, and the total cross section Σ relative to the collision outcome, compared to the experimental cross section Σ_{exp} at T=80 K (see Ref. 1).

	20 eV			95 eV	
	0°	15°	35°	0°	15°
Ag in adlayer	5.3	5.7	6.0	2.3	2.5
Ag in first layer	1.7	1.3	1.0	3.6	3.4
Ag in second layer	0.0	0.0	0.0	1.0	0.9
Ag in third layer	0.0	0.0	0.0	0.1	0.1
Pd adatoms	1.7	1.3	1.0	4.8	4.3
Vacancies	0.0	0.0	0.0	1.0	1.1

TABLE II. Correlation between the fragmentation of the cluster, described by the parameter $\langle r \rangle$, and the total cross section Σ relative to the collision outcome, compared to the experimental cross section Σ_{exp} at T=80 K (see Ref. 1).

	20 eV			95 eV	
	0°	15°	35°	0°	15°
$\langle r \rangle$ [Å]	1.2	1.3	2.7	2.4	2.7
Σ ($\sigma_{Pd(100)}$)	47.3	49.7	70.9	79.4	80.2
Σ_{exp} ($\sigma_{Pd(100)}$)		101.5		88.5	

In Ref. 1, the number of substitutional impurities at each incidence energy was estimated with the help of a simple model of implantation and fragmentation, assuming that the Ag adatoms were located at mutual distances exceeding the characteristic dimension of their cross section, and that the implanted Ag atoms were located as close as possible to the impact point. Under these hypotheses the number of Ag adatoms is equal to six at impact energy E_1 and ranges between three and four at E_2, while the number of substitutional Ag atoms is one at E_1 and between three and four at E_2. These data are in good agreement with the results of the simulations, as shown in Table I. It is possible to further pursue the comparison with the experimental results, by assigning a cross section to each simulated collision. This is easily done by attributing to each point defect (adatom, vacancy, substitutional impurity) produced at one collision, a cross section of the same magnitude, and estimating the total cross section by geometrical overlap of the individual cross sections. The obtained averaged cross sections are compared to the experi-

mental cross sections in Table II. In order to relate the cross sections to the observed fragmentation, we also report the parameter $\langle r \rangle$, which is the calculated mean distance to the center of mass of the cluster atoms. Very good agreement is found between the experimental cross section and the one that is estimated from the simulations at E_2. On the other hand, at E_1, the experimental cross section is twice as large as the cross section obtained from the simulations, at least at normal incidence and at $\vartheta = 15°$. This result is essentially unchanged by the introduction of an internal temperature of the cluster as high as $T = 1000$ K. We found this temperature to be the largest compatible with the existence of a bound liquidlike cluster prior to evaporation.

IV. DISCUSSION

Our findings can be interpreted within the mechanism diagram for the interaction between colliding clusters and surfaces of metal atoms proposed in Fig. 14 of Ref. 2. In that paper, the key quantities used to describe the effect of the impact were identified as being the ratio x between the cluster E_c^{clu} and the substrate E_c^{sub} cohesive energies and the ratio y between the cluster impact energy $E_{\mathrm{kin}}^{\mathrm{clu}}$ per atom and E_c^{sub}. In the case of Ag/Pd these values are $x = 0.45$, and $y_1 = 0.45$, $y_2 = 3.47$ for the two impact energies E_1 and E_2, respectively. Our EAM calculations are able to reproduce the experimental trend when $y = y_2$, with a strong evidence of implantation and dissociation, as predicted in the left part of the diagram of Ref. 2, which refers to $x < 1$. For $y = y_1$, the observed behavior resembles wetting more than dissociation, as found by comparing the calculated with the experimental cross sections. Therefore, the EAM modeling of the collision process appears to underestimate the stiffness of the substrate, and consequently it overestimates the ratio x. As shown by the location of the frontier between the region of dissociation and that of wetting in the xy plane (see again Fig. 14 of Ref. 2), this consequence is more severe for smaller values of the impact energies, thereby leading to the low values of the cross sections obtained in this work via EAM simulations.

In conclusion, we believe the results obtained can be highly useful, since they allowed us to capture relevant details of the collision process and complement the experimental results, by providing direct interpretations of cluster-collision data. This should stimulate further investigations in this area, in order to account in a manageable way for some of the more complex dynamical phenomena not included in the EAM description of energetic cluster interactions with surfaces.

ACKNOWLEDGMENTS

We are grateful to Professor J. Buttet and Dr. W. Harbich for stimulating discussions and constant encouragement. This work was supported by the Swiss National Fund for Scientific Research, with Grant No. 20-40736.94.

*Author to whom correspondence should be addressed. Present address: IPCMS-GEMME, 23 rue de loess, F-67037 Stresboug.

[1] G. Vandoni, C. Félix, R. Monot, J. Buttet, and W. Harbich, Chem. Phys. Lett. **229**, 51 (1994).

[2] H. Hsieh, R. S. Averback, H. Sellers, and C. P. Flynn, Phys. Rev. B **45**, 4417 (1992).

[3] F. Karetta and H. M. Urbassek, J. Appl. Phys. **71**, 5410 (1992).

[4] H. Haberland, Z. Insepov, and M. Moseler, Phys. Rev. B **51**, 11 061 (1995).

[5] S. M. Foiles, M. I. Baskes, and M. S. Daw, Phys. Rev. B **33**, 7983 (1986).

[6] W. Eckstein, *Computer Simulation of Ion-Solid Interactions*, Springer Series in Materials Science Vol. 10 (Springer-Verlag, Berlin, 1991).

[7] V. Bonacic-Koutecky, L. Cespiva, P. Fantucci, and J. Koutecky, J. Chem. Phys. **98**, 7981 (1993).

[8] A. F. Wright, M. S. Daw, and C. Y. Fong, Phys. Rev. B **42**, 9409 (1990).

[9] G. L. Kellogg and A. F. Voter, Phys. Rev. Lett. **67**, 622 (1991).

[10] C. Massobrio and P. Blandin, Phys. Rev. B **47**, 13 687 (1993).

[11] P. Blandin, C. Massobrio, and P. Ballone, Phys. Rev. Lett. **72**, 3072 (1994).